

Consistency Set Estimation for PET Image Reconstruction¹

Alfred O. Hero III*, Yong Zhang**, W. Leslie Rogers**

*Dept. of Electrical Engineering and Computer Science and **Division of Nuclear Medicine
The University of Michigan, Ann Arbor, MI 48109

Invited Paper

ABSTRACT

We give a method for determining a set of images which are consistent with measured projections data and error bounds on the projections noise. The error bounds can account for both statistical noise uncertainty and model uncertainty, e.g. due to a mismodeled or uncalibrated system matrix. If one knows the statistical distribution of the projections errors, then one can select the error bounds to give a consistency set which is a $(1 - \alpha)\%$ confidence region on the true image given the measured data. This region is a "set estimate" of the image which can be used to study confidence levels of popular image reconstructions such as filtered back projection, weighted-least-squares, and maximum likelihood. Alternatively, the set estimate can be used as a feasibility region from which particular image estimates can be selected based on additional criteria. We provide some numerical results for parallel ray projection geometries with Poisson projection statistics.

I. INTRODUCTION

Tomographic reconstruction can be stated in terms of estimating an image intensity $\underline{\lambda} \in \mathbb{R}^p$ from N measurements $\underline{y} = A\underline{\lambda} + \underline{\epsilon}$ where A is an $N \times p$ tomographic system matrix and $\underline{\epsilon}$ represents errors in the linear model $\underline{y} = A\underline{\lambda}$ due to noise or system mismodeling. A *point estimator* of $\underline{\lambda}$ is a point $\hat{\underline{\lambda}} = \hat{\underline{\lambda}}(\underline{y})$. The maximum likelihood via EM (MLEM), weighted-least squares (WLS), algebraic reconstruction technique (ART), and filtered back projection (FBP) are examples of point estimation strategies. While some of these point estimators may be derived based on some heuristic or statistical optimality criterion, for a given realization a point estimator does not provide any information about its statistical confidence or about its consistency with properties of the projection noise distribution. Such properties may be strongly parametric characterizations, e.g. known Poisson or Gaussian noise statistics, or they may be weaker

non-parametric characterizations, e.g. upper bounds on the α and $1 - \alpha$ quantiles of the noise distribution ($\alpha \in [0, 1]$). The quantiles can be used to develop a confidence region on the true image given the measured data set, and they have the advantage of less sensitivity to the accuracy of the assumed noise model than a detailed parametric description. Non-parametric characterizations may be especially useful for cases where a statistical model for noise and modeling errors are difficult to specify, e.g. due to calibration errors, detector latent response, randoms correction or detector dead-time.

This paper develops methods to obtain sets of consistent images based on the quantiles of the projection noise distributions. Using our methodology we can specify a *set estimator* which corresponds to a statistical confidence region, e.g. a 95% region, for the true image. A point estimator which is selected from this confidence region on the basis of other criteria or other constraints has the property of being consistent with 95% of the projection noise variations. We present an ellipsoid parallel cuts (EPC) algorithm for constructing confidence regions for PET images. The EPC algorithm acts iteratively on each row (projection) of the system matrix A . The algorithm generates a set of PET images which is consistent with: i) the measurements; ii) and upper and lower error bounds. A typical PET system has a sparse A matrix with a large number of rows, e.g. > 3000 is typical. Due to this structure we can significantly accelerate the EPC algorithm by performing a QR decomposition on the A matrix and implementing the EPC algorithm on the non-zero rows in the upper triangular system matrix that results from QR. Using this modified EPC algorithm and a variance stabilizing transformation on the projections data, we can generate confidence regions for PET images. We numerically implement QR-EPC to generate a consistency set which corresponds to a 95% confidence region for a simple PET phantom. We determine that the MLEM, the minimum MSE MLEM, and Llacer's stopped MLEM, all lie within the 95% confidence region. We also conclude that the negative-truncated centroid of the 95% consistency set is a point estimator whose quality is competitive with

¹This research was supported in part by the National Science Foundation under grant BCS-9024370 and the National Cancer Institute under grant R01-CA-54362-02

where Q is an $N \times N$ orthogonal matrix, i.e. $Q^T Q = \mathbf{I}$. Q can be obtained via a composition of Householder reflections of the columns of A [4]. By applying Q^T to both sides of the measurement equation $\underline{y} = A\lambda + \underline{\epsilon}$ we obtain:

$$\tilde{\underline{y}} = Q^T \underline{y} = Q^T A\lambda + Q^T \underline{\epsilon},$$

or equivalently:

$$\begin{bmatrix} \tilde{\underline{y}}_p \\ \tilde{\underline{y}}_{N-p} \end{bmatrix} = \begin{bmatrix} R \\ O \end{bmatrix} \lambda + \begin{bmatrix} \tilde{\underline{\epsilon}}_p \\ \tilde{\underline{\epsilon}}_{N-p} \end{bmatrix}$$

Notice that Q^T rotates components of the noise $\underline{\epsilon}$ lying outside the range space of A into the lower $N - p$ elements of $Q^T \underline{\epsilon}$, hence reducing the number of non-zero rows $\tilde{\underline{\epsilon}}_k^T$ from N to p . Discarding the last $N - p$ zero rows of the above measurement equation, we obtain the $p \times p$ system:

$$\tilde{\underline{y}}_p = \begin{bmatrix} R \\ O \end{bmatrix} \lambda + \tilde{\underline{\epsilon}}_p$$

Thus the QR-EPC algorithm converges in p steps instead of N steps to the final ellipsoid. One must weigh this savings against the cost of additional offline preprocessing ($A \rightarrow QR$) and online processing ($\underline{y} \rightarrow Q^T \underline{y}$, $\underline{\epsilon}_{min} \rightarrow Q^T \underline{\epsilon}_{min}$, and $\underline{\epsilon}_{max} \rightarrow Q^T \underline{\epsilon}_{max}$). The cost of offline computation of Q and R for a given A is $2p^2(N - p/3)$ flops if Householder reflections are used. This may be significantly reduced by using Given's rotations instead of Householder reflections if the A matrix is very sparse. In the Householder case, the online preprocessing cost is $(8Np - 4p^2)$ flops if symmetric noise bounds are used ($\underline{\epsilon}_{min} = \underline{\epsilon}_{max}$). We conclude that the total online cost of QR-EPC becomes $(4p^3 + 25p^2 + 21p + 8Np)$ flops. Since the matrix Q is needed, there is also an increase in the memory storage requirements for QR-EPC as opposed to regular EPC. Storage of the matrix Q requires $O(Np)$ Bytes if Householder reflections are used, whereas it requires only $O(\rho Np)$ bytes if Given's rotations are used, where $\rho \in [0, 1]$ is the sparsity factor of A .

For comparison the general (no exploitation of sparse A) MLEM algorithm needs $N(2p^2 + 2p)$ flops per iteration and may in some cases require several thousand iterations to converge. If N is twice as large p , the time to compute all p iterations of QR-EPC will be comparable to the time to compute a single iteration of general MLEM.

CONFIDENCE REGIONS

When $\underline{\epsilon}_{max}$ and $\underline{\epsilon}_{min}$ are selected to correspond to specific quantiles of the projection noise distribution the consistency set can often be manipulated to yield

a $(1 - \alpha)\%$ confidence region for $\underline{\theta}$. If a point estimator $\hat{\underline{\theta}}$ is outside of the consistency set the Euclidean distance between $\hat{\underline{\theta}}$ and the set E_p is simply:

$$\delta = (\hat{\underline{\theta}} - \underline{\theta}_p)^T \Sigma_p^{-1} (\hat{\underline{\theta}} - \underline{\theta}_p) - 1 \quad (5)$$

The distance $\delta + 1$ is called the *EPC distance*, which is a weighted distance between $\hat{\underline{\theta}}$ and the centroid $\underline{\theta}_p$ of E_p where the weight matrix is equal to Σ_p^{-1} . When the EPC algorithm is implemented on the noisy projections data, this distance measure can be used as a measure of consistency of an image reconstruction $\hat{\underline{\theta}}$ with a 95% confidence region for $\underline{\theta}$. For example, it could be used as a stopping rule for ML-EM or other iterative reconstruction algorithm much in the same manner as the H function of Llacer [5]. Alternatively, one can run the EPC algorithm on the noiseless data \underline{y} to obtain an ellipsoidal region, called the *centered consistency set*, centered at the true $\underline{\theta}$. This region indicates the natural variations which can be expected of a good unbiased image reconstruction which are induced by variations in the projection noise.

III. NUMERICAL STUDIES

A phantom with intensity λ sampled over 26×32 pixels (Fig. 1) was projected onto 42 detector bins at 90 equally distributed angles using strip integrals to form 3780 mean projections $A\lambda$. Using these mean projections as Poisson rates, the projection data was generated as 3780 independent Poisson random variables. Using the square root variance stabilizing transformation on the projections data \underline{y} it can be shown that $2(\sqrt{\underline{y}} - \sqrt{A\lambda})$ is approximately distributed as a vector of i.i.d. $\mathcal{N}(0, 1)$ (standard normal) random variables. Let Z_α denote the $\alpha\%$ quantile of the $\mathcal{N}(0, 1)$ distribution. Using this fact, and assuming that $\sqrt{y_i} \geq \frac{1}{2}Z_{(1-\alpha/2)^{1/N}}$, a $1 - \alpha$ confidence rectangle for $A\lambda$ is obtained as $\times_{i=1}^p [\beta_{min}(i), \beta_{max}(i)]$ where $\beta_{min}(i) = (\sqrt{y_i} - \frac{1}{2}Z_{(1-\alpha/2)^{1/N}})^2$ and $\beta_{max}(i) = (\sqrt{y_i} + \frac{1}{2}Z_{(1-\alpha/2)^{1/N}})^2$. From this we obtain a $(1 - \alpha)\%$ confidence region for $\underline{\lambda}$:

$$\Lambda_{1-\alpha} = \{ \underline{\lambda} : \underline{\epsilon}_{min} \leq \underline{y} - A\lambda \leq \underline{\epsilon}_{max} \} \quad (6)$$

where

$$\begin{aligned} \underline{\epsilon}_{min} &\stackrel{def}{=} \underline{y} - \underline{\beta}_{max} \\ \underline{\epsilon}_{max} &\stackrel{def}{=} \underline{y} - \underline{\beta}_{min}. \end{aligned}$$

This is in a form suitable for application of the QR-EPC algorithm.

We implemented the QR-EPC algorithm for a 95% confidence region by setting $1 - \alpha = 0.95$ in (6). The

algorithm was initialized with a spheroid E_0 of radius 10^6 . The MLEM algorithm was also implemented, without regularization or smoothing, to produce a sequence $\hat{\lambda}^i$ of image estimates converging to the ML estimate. The EPC distance $(\hat{\lambda}^i - \theta_p)^T \Sigma_p^{-1} (\hat{\lambda}^i - \theta_p)$, the Euclidean distance $MSE = (\hat{\lambda}^i - \lambda_o)^T (\hat{\lambda}^i - \lambda_o)$, and Llacer's H -distance for feasible images [5] have been plotted as a function of MLEM iteration i in Figs. 4, 2 and 3 for 1.3 million counts. Note that the EPC curve is monotone decreasing from iteration 1 to iteration 1000. Since the EPC curve falls below the threshold of 1.0 at iteration 7, the MLEM iterates are within the 95% confidence region thereafter. This monotonicity indicates that MLEM is converging into the vicinity of the centroid image. The MSE curve decreases to a minimum at the 21-st iteration, at which point the MLEM iterate is closest to the phantom in Euclidean distance, and sharply increases thereafter. The H curve decreases to a minimum at the 37-th iteration, at which point the likelihood that a Poisson mechanism could have produced the projections data is maximum, and increases in a jagged manner thereafter. If adopted as stopping rules, Llacer's H function would stipulate that the MLEM be stopped at iteration 37 while the EPC distance function would stipulate that MLEM be iterated beyond 1000. For 2.6 million counts the Euclidean distance and Llacer's H have been plotted in Figs 2-6. The minima of these two functions are less pronounced than in the lower count regime and they occur at a larger iteration index. As in the 1.3 million count case, the behavior of the EPC distance is monotone decreasing and the plot has been omitted.

In Figures 7 and 8 minimum MSE, Llacer's stopped MLEM, (300 iteration) MLEM, and EPC centroid images are displayed for the cases of 1.3 and 2.6 million counts, respectively. A non-negativity constraint was imposed on the centroid images by truncating negative values to zero. Note that the visual quality of the constrained EPC centroid image is comparable to that of MLEM. Both the EPC and the MLEM algorithms were run on a Stardent 3000 machine. MLEM required 10 mins. of CPU time for 1000 iterations while QR-EPC required 5 mins. of CPU time, including the setup time for rotating the vectors \underline{y} , \underline{e}_{max} , and \underline{e}_{min} , to run.

The concentration matrix Σ_p characterizes the coupling among the pixels in the 95% confidence region induced by the shape of the final ellipsoid. The coupling between a particular pixel and the rest of the image pixels is indicated by a column of Σ_p and can be represented as a coupling map shown in Fig. 9 for 3 representative pixels in the phantom image. These pixels have been selected as the center points of the three hot spots in

the phantom image and are the bright pixel in each of the three coupling images in Fig. 9. The brightness of this pixel is the variance, i.e. the extent of the confidence interval, in that pixel's intensity. The brightness of other pixels in the parameter coupling maps represent the degree to which the bright pixel is coupled to the other pixels through the shape of the consistency set. For example, a delta function in any of these parameter coupling maps would indicate that the bright pixel varies independently of the other pixels within the 95% confidence region.

References

- [1] R.G. Bland, D. Goldfarb and M.J. Todd, "The Ellipsoid Method: A survey", *Operation Research*, vol. 29, No.6, pp. 1039-1091, 1981.
- [2] P. L. Combettes and H. J. Trussell, "The use of noise properties in set theoretic estimation," *IEEE Trans. Signal Processing*, Vol. 39, No. 7, pp. 1630-1641, 1991.
- [3] E. Fogel and Y. Huang, "On the value of information in system identification -bounded noise case," *Automatica*, vol. 18, pp. 229-238, 1982.
- [4] G. Golub and F. Van Loan, "Matrix Computation", 2nd edition, Johns Hopkins University Press 1989.
- [5] J. Llacer and E. Veklerov. "Feasible Images and Practical Stopping Rules for Iterative Algorithms in Emission Tomography," *IEEE Trans. Med. Imaging*, pp. 186-193, June 1989.
- [6] M. Milanese and R. Tempo, "Optimal algorithms theory for robust estimation and prediction" *IEEE Trans. Automat. Control*, Vol. AC-30, 730 - 738, 1985.
- [7] F. C. Schweppe, "Recursive state Estimation: Unknown but bounded error and system inputs," *IEEE Trans. Automatic Control*, vol. AC-13, pp. 22-28, 1968.
- [8] R. Tempo and A. Vicino, "Optimal algorithms for system identification: A review of some recent results," *Math. Comput. Simulat.* vol. 32, 1990, 585-595.
- [9] E. Walter and P. Lahanier, "Estimation of Parameter Bounds from Bounded-Error Data - A survey," *Math. and Comp. Simulat.*, vol. 32, pp. 449-468, 1990.

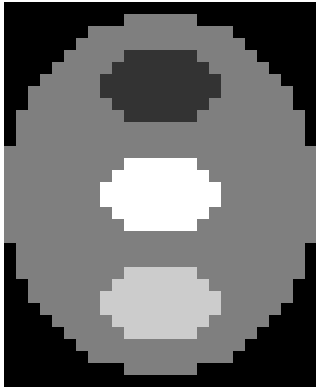


Figure 1: Phantom Image

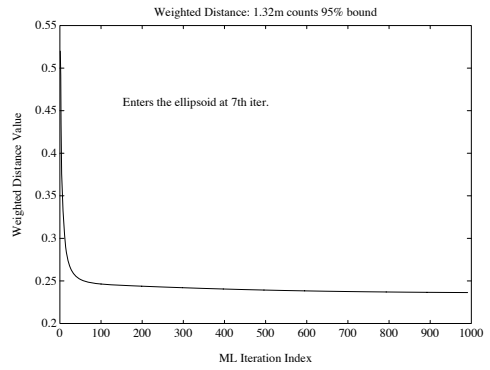


Figure 4: EPC distance curve for 1.3M counts

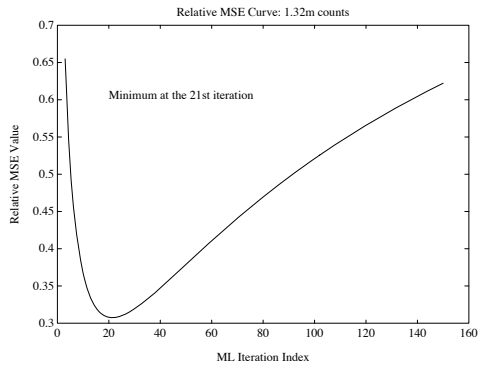


Figure 2: MSE Curve for 1.3M Counts

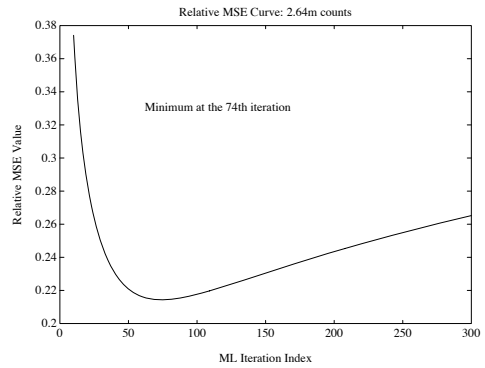


Figure 5: MSE Curve for 2.6M Counts

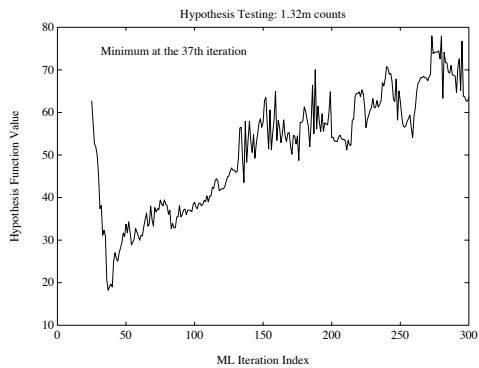


Figure 3: Llacer's H Curve for 1.3M Counts

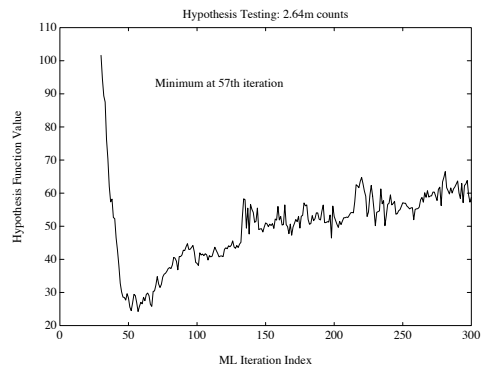


Figure 6: Llacer's H Curve for 2.6M Counts

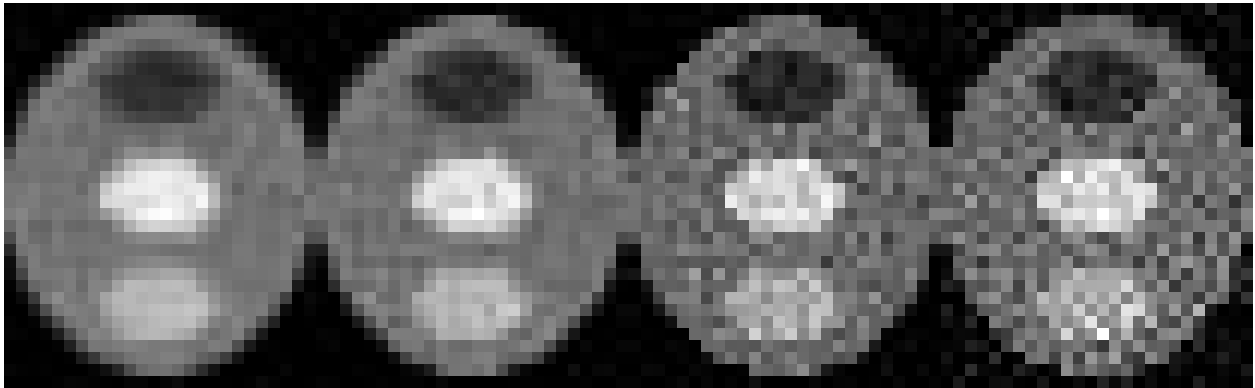


Figure 7: Min MSE, Llacer stopped MLEM, unstopped MLEM, constrained EPC centroid, for 1.3M counts

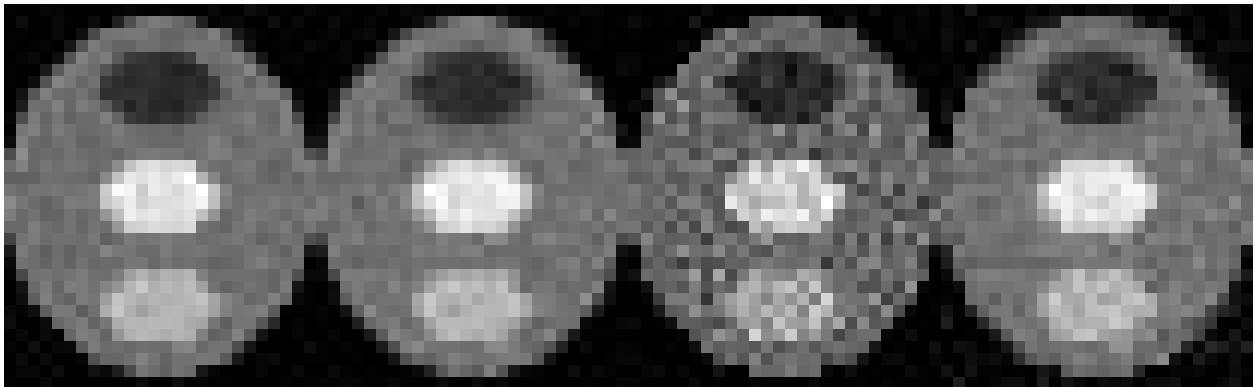


Figure 8: Min MSE, Llacer stopped MLEM, unstopped MLEM, constrained EPC centroid, for 2.6M counts

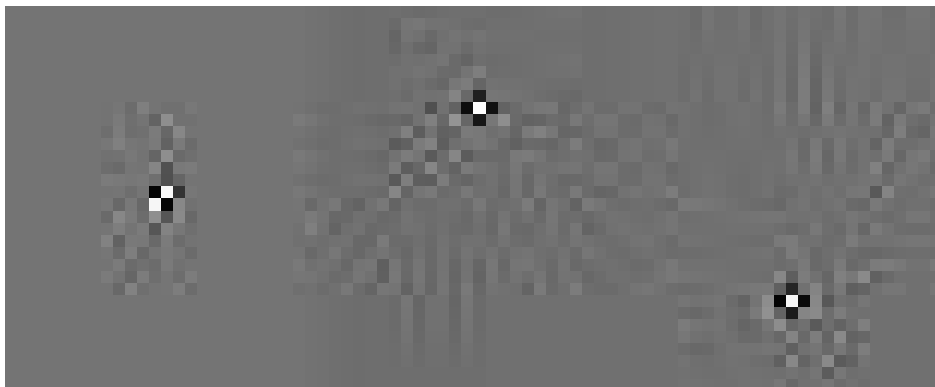


Figure 9: Coupling image for various pixels